M-Type Hexaferrites Its Types And Possible Application

Majahid Ul Islam[a] , Shahnaz Kossar[a]* & Raj Paul[b]

[a,a*,b] Department of Physics , GNA University , Sri Hargobindgarh, Pa

hagwara- Hoshiarpur Road, Phagwara , Punjab-144401

Corresponding author * Email: shazia.rajput0505@gmail.com

Abstract

In the recent year, the hexaferrite of the M-type has attracted a lot of attention due to its excellent magnetic properties, its high coercivity value, its exceptionally good chemical stability, corrosion resistance, and its high Curie temperature. Due to these exceptional properties M Type hexaferrite is used for many applications. In the present work, we have explained different types of hexaferrite especially M types hexaferrite their properties, and corresponding structure Hexaferrites like BaM, SrM, and PbM exhibit excellent properties that allow them to be used for microwave absorbers, media recorders, and other biomedical applications.

Introduction

Materials science has played a key role in shaping and development of civilizations since the dawn of time . With the development of materials science, it is recognized as a specific field of science and engineering development with economic growth are the main factors [1]. In the 1950s, the material science research based on silicon industrial revolution had a profound impact on and transformed our society by enabling the emergence of the technologies of today [2]. Such as wireless communications, mobile phones, data storage (digital) and widespread electronics appliance [3,4,5]. Today's emerging topics in material science and technology includes nano-materials[6], spintronic materials[7], bio-materials [8,9], carbon nano-tubes, graphene , multiferroic materials[11], smart and advanced functional materials, capable to bring a new wave of advanced technology as compare to the industrial revolution of 1950s. Over the past 15 years, multiferroic materials have become increasingly popular due to their interesting physical and chemical properties which make them suitable for technological applications [12,13].

Multiferroic materials are the type of solid-state compounds that possesses more than one order of states such as ferromagnetism, ferroelectricity, ferroelasticity, and ferrotoroidicity

within one phase [14,15,16]. Such types of multiferroics were able to display strong piezo-electric, piezo-magnetic as well as magneto-elastic and electro-elastic properties [17]. Both of these materials (ferromagnetic and ferroelectric) are essential for technological applications because they can control both ferroelectric and ferromagnetic properties via external mechanical stress due to the coupling between the phases [18,19,20].

Moreover, the converse effect is also applied in magnetic and electric fields to modify the shape of the material by introducing mechanical strain. Fig. 1 illustrates the complex coupling between magnetization - magnetic field - strain, electric polarization - electric field - strain, and stress - strain - electric polarization - magnetization.

The coexistence of ferro-order and piezo-elastic properties can produce intriguing piezo-electric and piezo-magnetic couplings. It is important to note that by the electric and magnetic order states, any ferroic order can be observed, including ferromagnetic, antiferromagnetic, ferri-magnetic, and paramagnetic orders, as well as their electrical equivalents. In addition to their ability to exhibit numerous order states, what fascinates scientists about multiferroic materials is their ability to show cross-coupling effects between them.

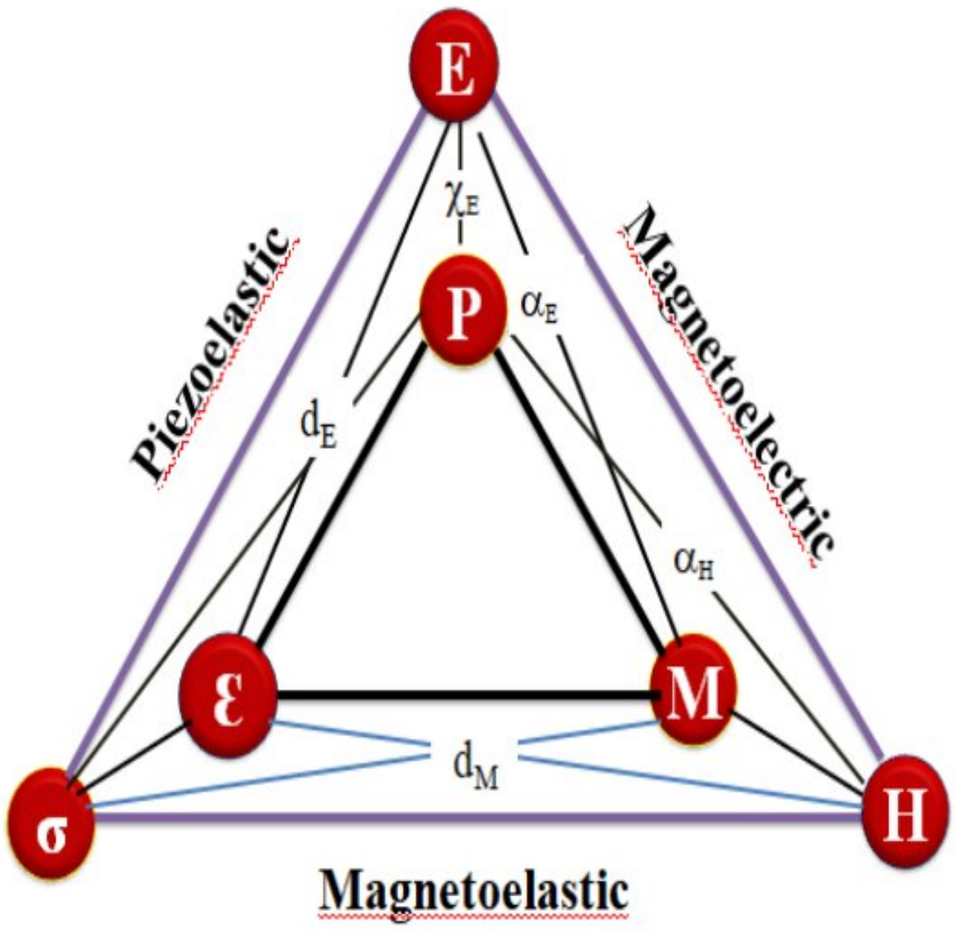

Figure 1. Illustration of magnetic – elastic - electric coupling properties in multiferroic material exibiting order parameters (M, P and ε) and conjugate fields E – electric field; σ - applied mechanical stress;; H – magnetic field. P – electric polarization; M – magnetization and ε - strain

In the hysteresis loops, we observe the maximum magnetization/polarization with applied magnetic/electric fields, coercive magnetic/electric fields, and residual magnetization/polarization, etc., which are used to describe ferroelectric and ferromagnetic materials. Figure 2 shows the common spin and dipole configurations and hysteresis loops in ferroelectric and ferromagnetic materials[21].

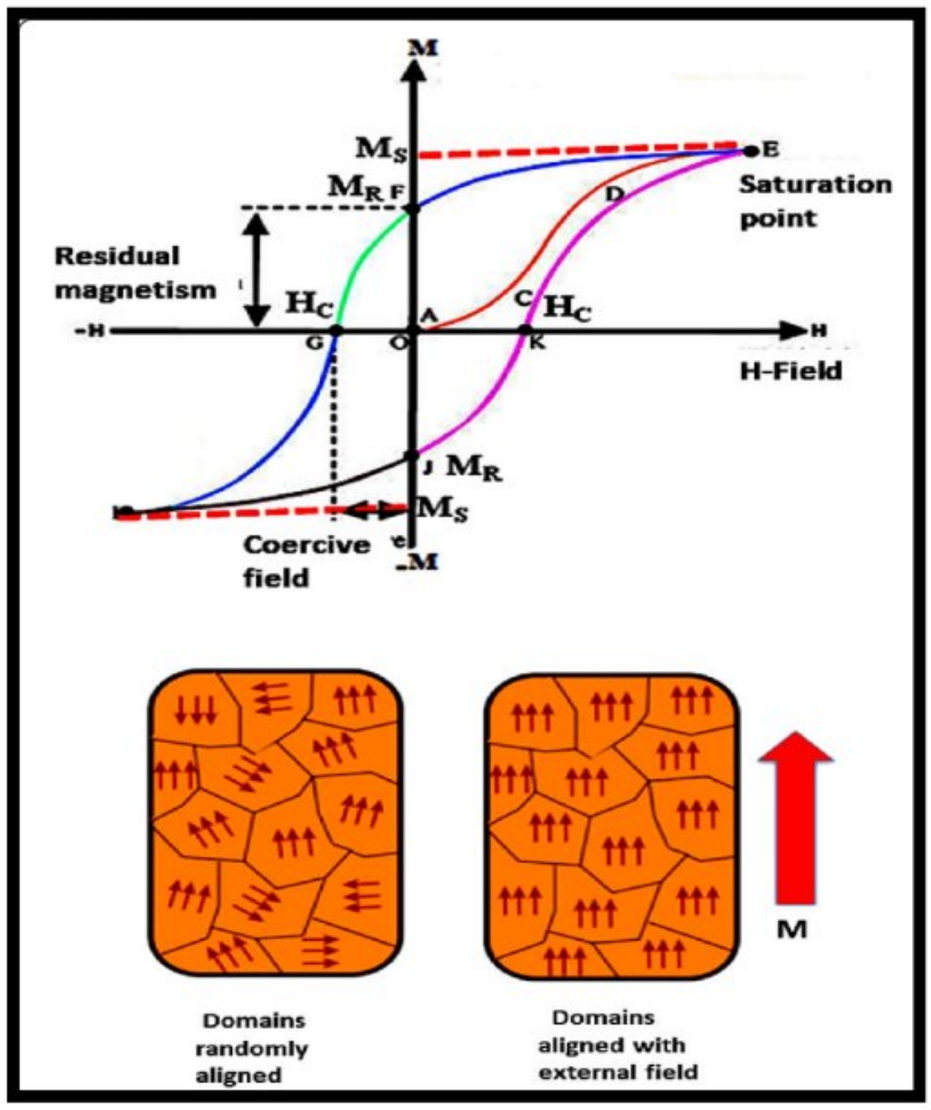

Figure 2 Ferromagnetic hysteresis loop and ordering of spins; M; Magnetization, H ;Magnetic field, P ; Electric polarization and E; Electric field [22].

Many ferroelectric and ferromagnetic materials have been reported in the literature, and they are now an important component of modern science and technology. For instance, ferroelectric material exhibiting induced switchable electric field, spontaneous electric polarizations are used in non-volatile ferroelectric memories. It has also been found that magnetic data storage devices and magnetic read/write heads of electronic devices are made from ferromagnetic materials. The coexistence of ferroelectricity and ferromagnetism in multiferrites makes them extremely appealing for a variety of technological applications. For

example, these materials are used in spintronics, where the manipulation of electron charge and spin is critical, Multiferrites can be used to make new memory devices, sensors, actuators, energy harvesting devices and also in biomedical applications[23]. Bismuth ferrite (BiFeO3), bismuth manganite (BiMnO3), barium nitrate(BaTiO3) , Barium ferrite (BaFeO3), and yttrium iron garnet ($Y_3Fe_5O_{12}$) are all examples of multiferrite minerals. Because of their multifunctional features and possible applications, these materials have attracted the curiosity of researchers. In this chapter we will focus on stracture and some of the best application of M type hexagonal ferritrs.

2 Stracture and properties of Hexagonal Multiferrites

Magnetoplumbite was described in 1925 [24], and its crystal structure was determined in 1938 to be hexagonal with the constituent Pb $Fe_{7.5}$ $Mn_{3.5}Al_{0.5}Ti_{0.5}O_{19}$ [25,12]. It was discovered that Magnetoplumbite is made from $PbFe_{12}O_{19}$ or pure PbM, and several isomorphous compounds were discovered including $BaFe_{12}O_{19.}$ Jonker et al. also found other compounds in heating the ternary BaO-Fe_2O_3-MeO system at 1200–1400 °C[26,27]. There are numerous types of hexagonal ferrites, sometimes known as hexaferrites. These hexaferrites are: M-type ferrites-Barium ferrite or BaM ($BaFe_{12}O_{19}$); W-type ferrites $BaCo_2Fe_{16}O_{27}$ Such as Fe_2W ($BaFe_2Fe_{16}O_{27}$); X-type ferrites $Ba_2Me_2Fe_{28}O_{46,}$ such as Co_2X ($Ba_2Co_2Fe_{28}O_{46}$); Y-type ferrites Ba2 $Me_2Fe_{12}O_{22}$, like Co_2Y ($Ba_2Co_2Fe_{12}O_{22}$); U-type ferrites $Ba_4Me_2Fe_{36}O_{60,}$ namely Co_2U ($BaCo_2Fe_{36}O_{60}$) and Z type ferrites-$Ba_2Me_2Fe_{24}O_{41}$, namely Co_2Z ($Ba_2Co_2Fe_{24}O_{41}$).

A divalent transition metal or other divalent cation is represented by "Me"[12,28], and all of these compounds possess a hexagonal crystal structure with two crystalline lattice parameters: a, the hexagonal plane width, and c, the hexagonal crystal height

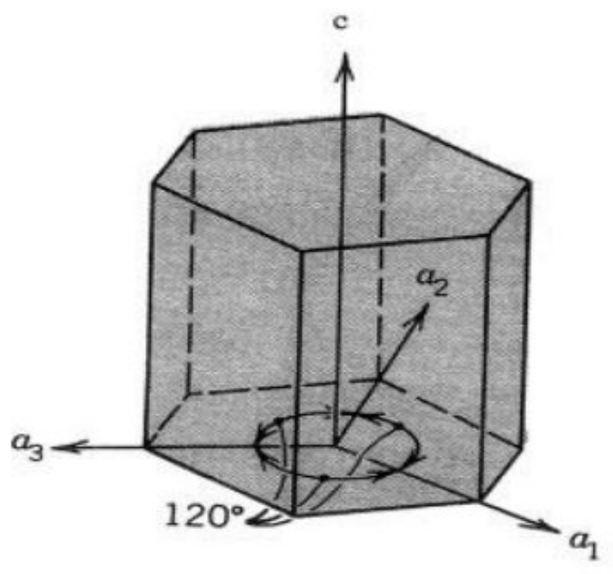

Figure 3: Hexagonal crystal, with lattice parameters represented by a & c. Adopted from [29].

The physical characteristics of different types of hexaferrite is shown in the table 1 .

Ferrites (Type)	Formulla	Molecular mass(g)	Density ρ (g/ cm)	c (Å)	Magnetisation (at room temperature)
BaM	$BaFe_{12}O_{19}$	1112	5.29	23.18	Uniaxial
SrM	$SrFe_{12}O_{19}$	1062	5.11	23.02	Uniaxial
Co_2W	$BaCo_2Fe_{16}O_{27}$	1577	5.31	32.84	In cone
Co_2X	$Ba_2Co_2Fe_{28}O_{46}$	2688	5.29	84.11	In Cone
Co_2Y	$Ba_2Co_2Fe_{12}O_{22}$	1410	5.40	4356	In plane
Co_2Z	$Ba_2Co_2Fe_{24}O_{41}$	2522	5.35	52.30	In plane
Co_2U	$BaCo_2Fe_{36}O_{60}$	3624	5.31	3816	In plane

Table 1: At room temperature, Some physical characteristics of different types of hexagonal ferrites [29].

M-type hexaferrites

Barium ferrite (BaM)

The compound BaM, $BaFe_{12}O_{19}$, were studied for the first time in the 1936 at a melting point of about 1390 °C [30,12]. The structure was not defined until Philips defined it magnetically in the early 1950s when the structure was found to be isomorphous to the hexagonal magnetoplumbite [29]. The ferrites were significantly cheaper to manufacture, having low saturation magnetization, had a high electrical resistance (10^8Ohm cm) , and had a high uniaxial magnetic anisotropy along the c-axis (17 kOe). The maximum density of BaM as a ceramic material is 5.295 g/cm^3, and its molecular mass is 1112 g / Mol [31], but in practice, it can be as low as 90% of its theoretical density. It has been estimated that BaM has a c-axis hardness of 5.9 GPa [32]. The hexagonal structure of barium ferrite with the space group P 63/mmc can be seen in Figure 4 [33,34]. This structure can be represented symbolically as RSR*S, where R denotes a 3-layer structure having two O_4 and BaO_3 with the composition $Ba^{2+}\ Fe_6^{3+}O_{11}^{2-}$, and S signifies a 2-layer structure containing two O_4 with the composition $Fe_6^{3+}O_8^{2-}$. The asterisk indicates the structure rotation of 180-degree about the c-axis.

Through optimizing the volume, shape, and internal coordinates of the hexagonal unit cell, Moitra et al found a = 5.35 A and c = 21.19 A as equilibrium lattice constants for the hexagonal

unit cell, which are in good agreement with observed values of a = 5.90 A and c = 23.24 A[35].

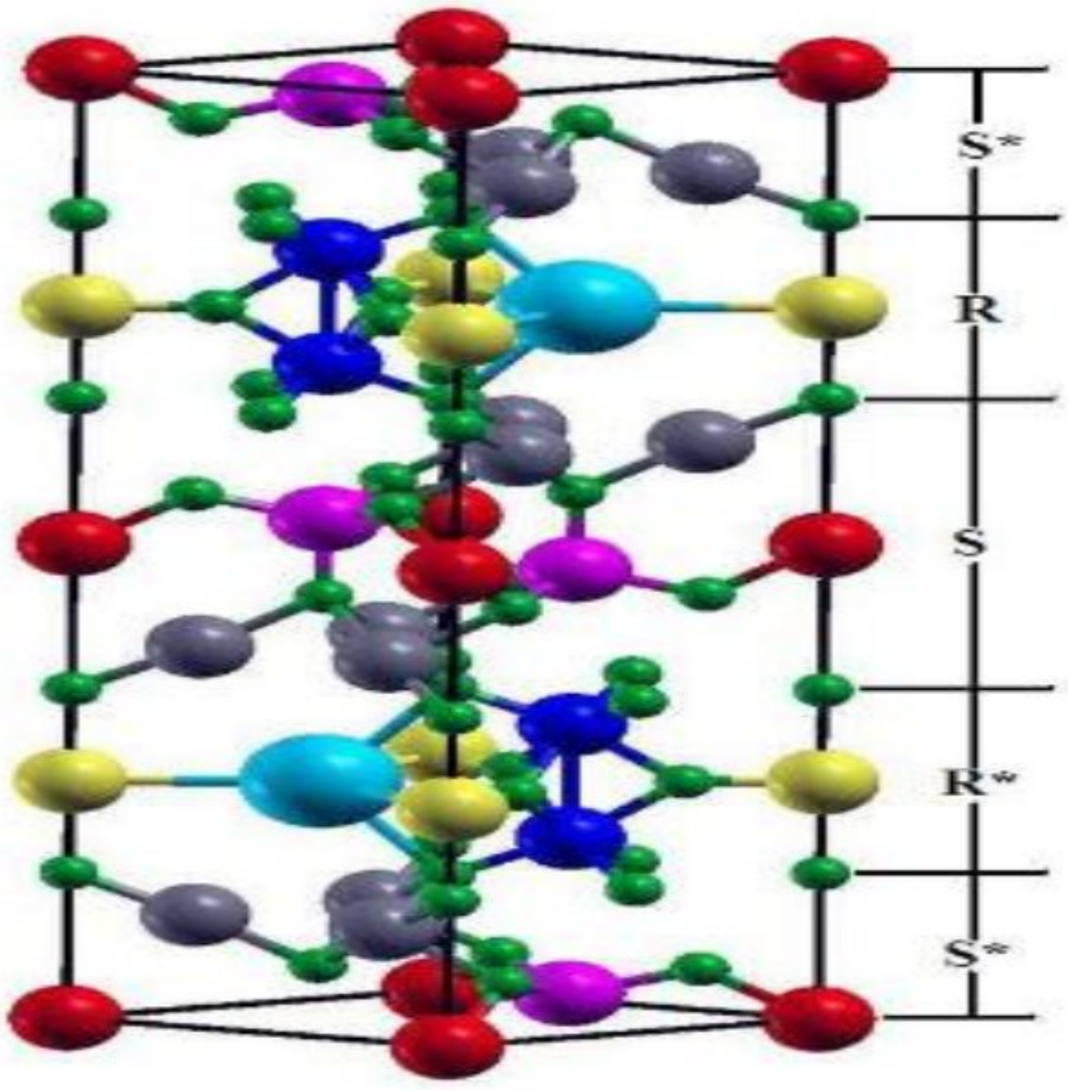

Figure 4: An overview of the structure of M type barium hexaferrite. There are different colors of spheres representing iron atoms at 2a, 12k, 4f1, 4f2, and 2b sites. A green sphere represents an oxygen atom, while a cyan sphere represents a barium atom. [35]

Strontium M-type hexagonal ferrite (SrM)

Strontium M type hexagonal ferrite (SrM) discovered by Cockherdt in 1963[36] , is a ferrite that belongs to the magnetoplumbite phase [29]. Due to the comparatively strong magnetocrystalline anisotropy field, The $SrFe_{12}O_{19}$ ferrimagnet have exceptional saturation magnetization (70 emu/g) as well as coercivity (6.64 kOe). [37,38,39].The standard and availability of raw materials, the comparatively low cost of manufacturing, the outstanding chemical stability and anticorrosion capabilities, and high Curie temperature of 470 °C are all advantages[40].

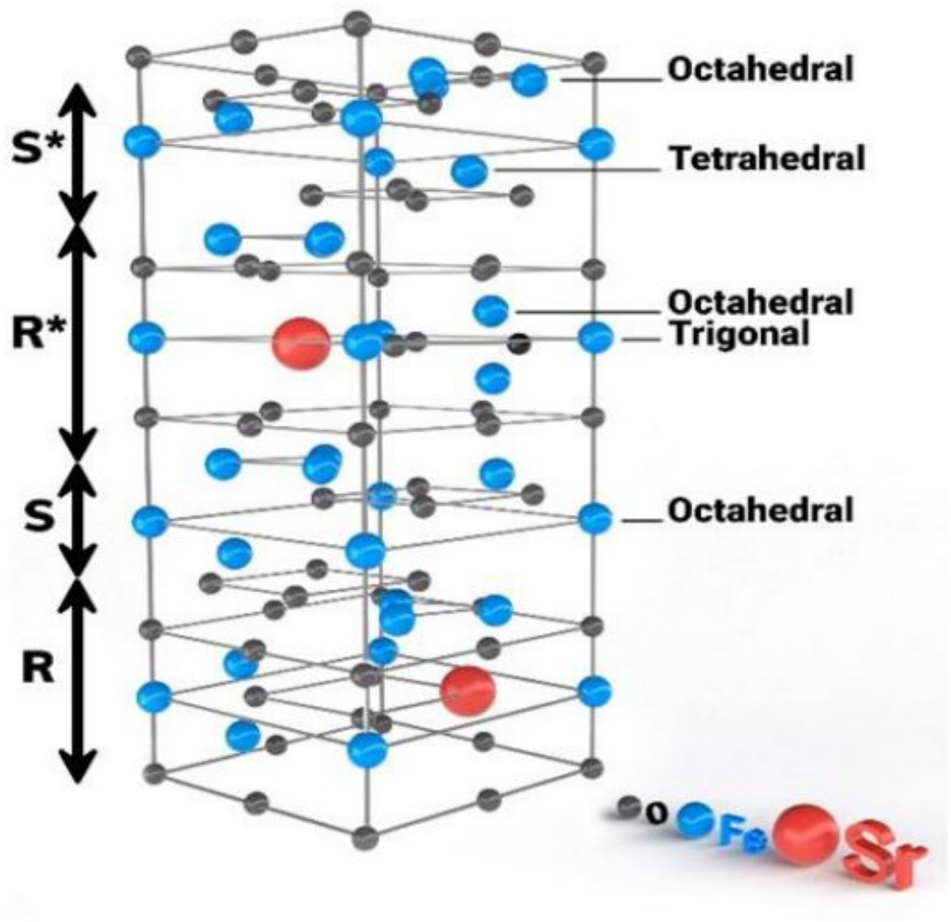

Figure 4: An overview of the structure of M type strontium hexaferrite SrM containing S and R block) adopted from [43].

There are four main block of SrM represented by RSR*S*, S being spinal = $Fe_6O_8^{2+}$ and R being hexagonal = $MFe_6O_{11}^{2-}$, which are hexagonal with a space group of P63/mmc [41,42]. There is an asterisk (*) beside each subunit denotes that the subunit has been rotated 180 degrees around the crystallographic c-axis. The total magnetization of the unit cell at absolute zero temperature is proportional to the number of Fe^{3+} ions.

In strontium hex ferrite SrM there is an equal distribution of Fe^{3+} ions between the two blocks. In the hexagonal structure of the R block, five ions are arranged in an octahedral pattern with three ions in spins up and two are in spins down of the magnetic moments, and one spin up on the bipyramidal site. Among the six Fe^{3+} ions in the S block with spinel structure, four are in the octahedral position. There is a spin-up moment for the atoms at the octahedral positions, while a spin-down moment for the atoms at the tetrahedral positions. In each block, three or more ions are distributed equally.

Due to these exceptional qualities, $SrFe_{12}O_{19}$ has found widespread use in a variety of technological applications, including magneto optics systems, electronics, electric motors, the telecommunications industry, microwave absorbers, magnetic recording, memory devices and sensors. [44,45,46,47,48].

Lead M-type hexagonal ferrite (PbM)

In M type hexaferrite family, lead ferrite is hard magnetic material with low synthesis and sintering temperatures. PbM has a molecular mass of 1181g, Which is much heavier than barium and strontium and a density of 5.708 g /cm^3[49].The Pb2+ ion size lies in between the barium and Strontium. Figure 1a depicts the structure of $PbFe_{12}O_{19}$. It is composed of spinel and hexagonal blocks, similar to other hexaferrites with magnetoplumbite structures. Along the c axis, Oxygen anions and large lead ions alternate in a 10 layer ABABACBCBC structure, with Pb2+ cations occupying the third and eighth layers. One unit cell includes two $PbFe_{12}O_{19}$ formula units. Pb^{2+} cations have an anticuboctahedral first oxygen coordination sphere (Figure 5b), However there are five different crystallographic positions of iron cations (Figure 1c-g): Fe1 (2a), Fe4 (4f1), and Fe5 (12k), respectively, octahedral, trigonal-bipyramidal, and tetrahedral.

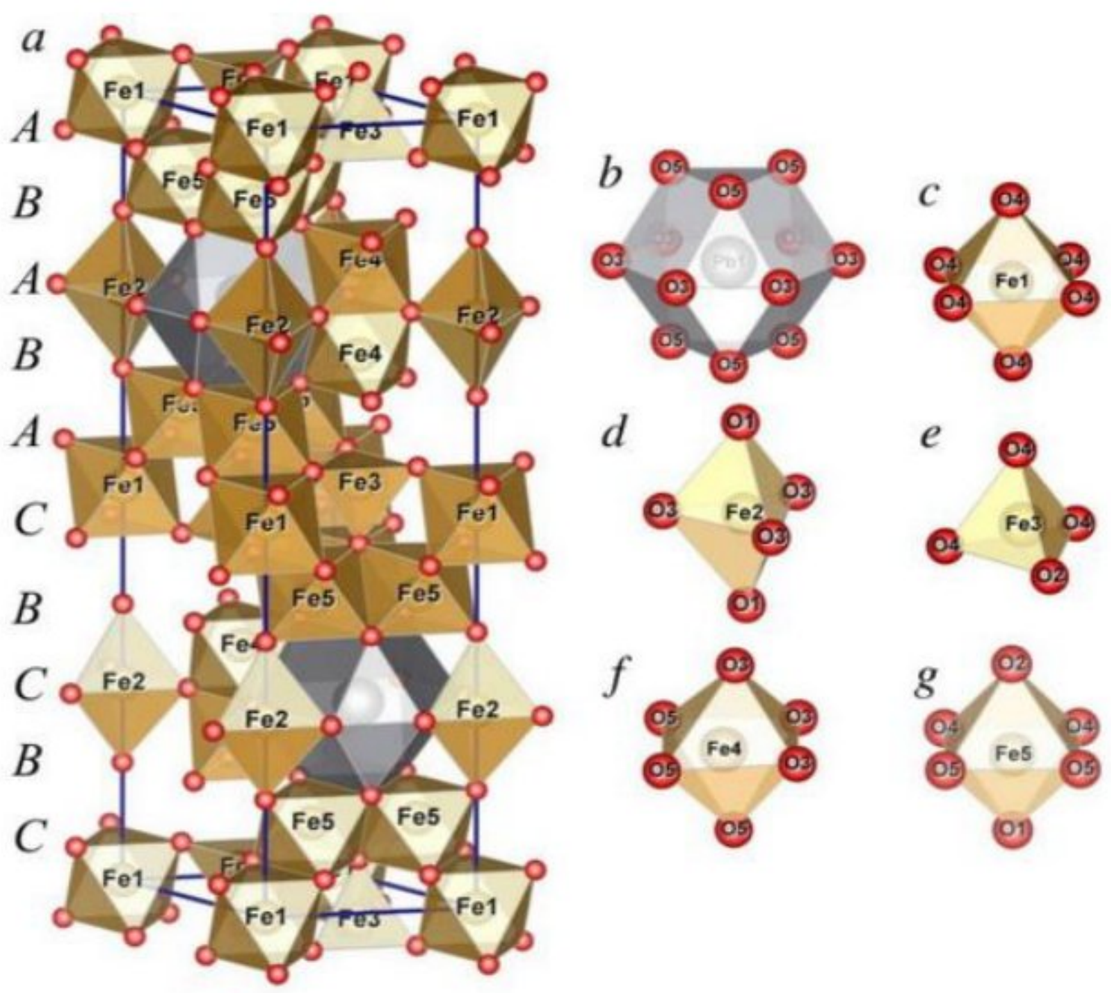

Figure 5. (a) Illustration of $PbFe_{12}O_{19}$ unit cell, (b) shows cations of Pb^{2+} and (c–g) shows cations of Fe^{3+} [50]

Table 2 shows physical properties along with the value of different parameter of BaM, SrM and PbM ferrites. d = density in g/cm^3[11]. T_m = melting point in Kelvin, whereas the average thermal expansion coefficients for volume and a and c axis are defined by αa , αc and αv. The symbols a and c are the lattice parameters, v defines cell volume and Tc is Curie temperature measured in K [29].

	δ	T_m	α_a	α_c	α_v	a	c	V	T_c
SrM	5.101	1692	8.62	16.08	33.50	5.8844	23.0632	691.6	732
BaM	5.295	1611	10.74	16.29	38.16	5.8876	23.1885	696.2	725
PbM	5.708	1538	10.80	18.34	40.46	5.8941	23.0984	694.9	718

Applications of M ferrites

M-type hexaferrite and related compounds have many applications due to their exceptional electric and magnetic properties. Some of the main application of M type hexaferrites are microwave absorber, magnetic recording, biomedical application like hyperthermia (cancer treatment) and high frequency electronic devices .

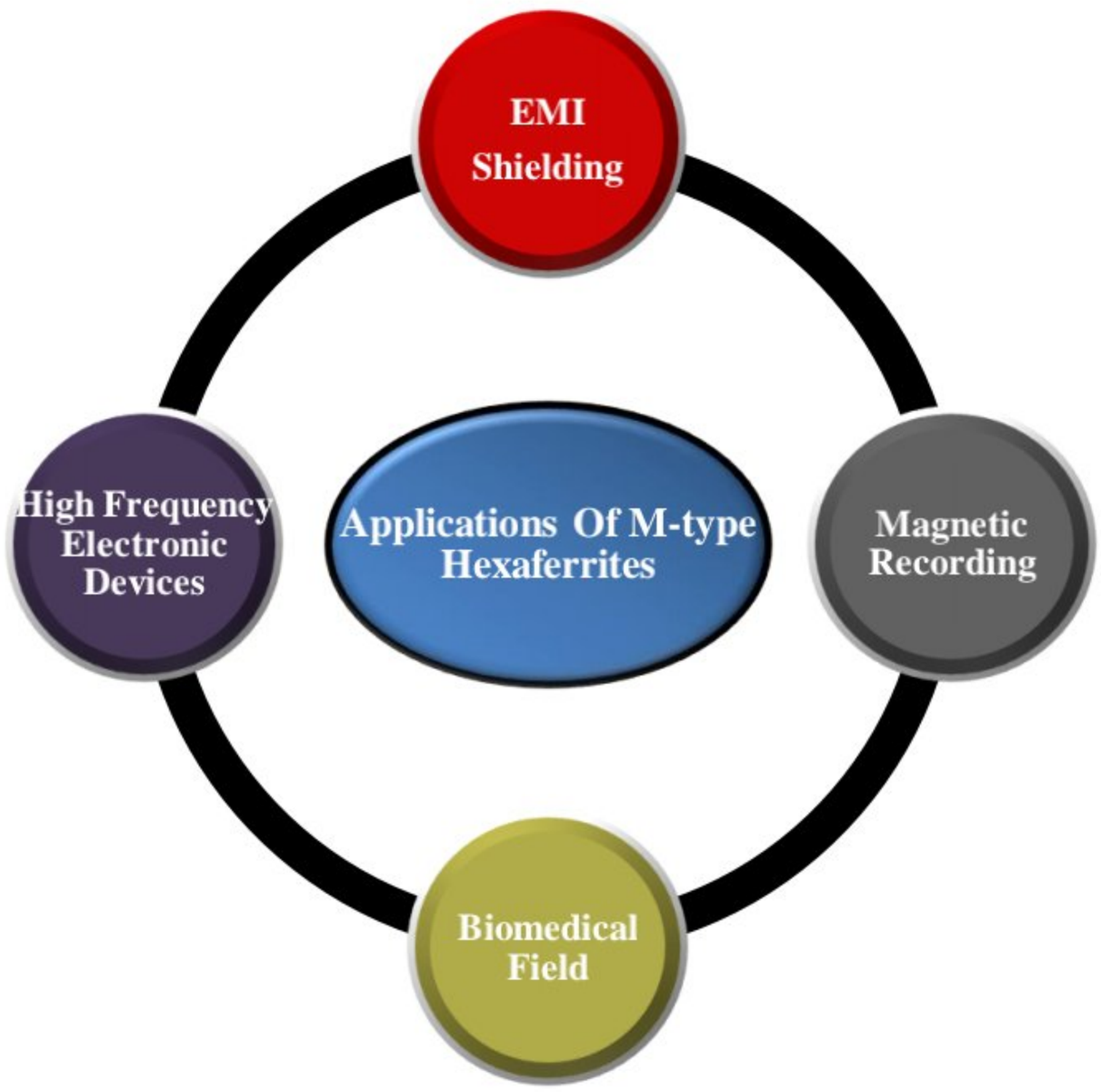

Figure 6: shows some of the application of M-type hexaferrites.

1. Electromagnetic Interference (EMI) Shielding.

For the uninterrupted operation of electronic appliances, the absence of electromagnetic interference is very crucial. This is achieved by using materials that should absorb electromagnetic radiation from all the sources [51]. In electromagnetic interference (EMI) shielding the radiations being shielded by absorption, reflection, or multiples reflections. This

method is also known as the microwave absorption method and is significantly more efficient than the other conventional process. Microwave sensing and communication are nowadays very essential components for defense and other industries, as a result of this there is an increased interest in using high-efficiency EM wave absorbers for secretive and shielding innovations. Good electromagnetic wave absorber materials possess a high absorption efficiency, a wide absorbing bandwidth, high resistivity, lower density, and a reasonable cost [52,53].

The materials like metallic oxides , metal particles , carbon materials ,ferrites, and conductive polymers are excellent EM wave absorbers due to their high absorption efficiency and other properties as mentioned above. The total shielding efficiency of these shielding materials can be expressed as the sum of absorption, reflection, and transmission coefficients and and can be expressed as [54]

$$S_E = S_{EA} + S_{ER} + S_{ET}.$$

Where the coefficients are expressed as

$$S_{EA}\ (dB) = 10 \log (1-R/T)$$

$$S_{ER}\ (dB) = 10 \log (1/T)$$

$$S_{ET}\ (dB) = 10 \log (1/1-R)$$

Many other mechanisms dominated by shielding from multiple reflections, i.e., reflections inside the material, and often they are neglected. Complex permittivity/permeability-frequency plots are used to evaluate the reliability of EMI shielding capacity of materials, especially absorption. A complex parameter is one that has real and imaginary parts. Real permittivity and permeability represent actual stored energy in the material. while the imaginary part represents the energydi ssipated in the form of heat.

.Amongs the multiferrite materials, M-type barium ferrite ($BaFe_{12}O_{19}$) is very useful in many real applications because of the ease of manufacture, nontoxic nature , and exceptionally economical. Due to its extraordinary magnetic loss caused by resonance, ferrite serves as a good microwave absorber [55]. The resonance frequency of $BaFe_{12}O_{19}$ is, however, reported by researcher around 43.5 GHz [56].

Therefore, it is necessary to modify the natural resonance frequency to the lower range in order to produce absorption within range of 2–18 GHz. Due to the direct correlation between the

natural resonance frequency of ferrites and magnetic anisotropy (HA), which is produced by exchange-coupling of Fe^{3+} ions in lattices. In place of Fe^{3+} ions, non-magnetic or weaker magnetic ions will decrease HA. The magnetic anisotropy (H_A), may be reduced more if the Fe^{3+} ions are being replaced. In addition, improving the complex permittivity of a material can also increase its microwave absorption efficiency by reducing reflection loss (RL) in the material after the natural resonance with the Fe3+ ions is replaced. Barrium ferrite co-doped with Zr^{4+} - Ni^{2+} [$BaFe_{12-2x}$ (Zr Ni) $_x$ O_{19}], were prepared by Zhang et.al and sintered these ferrites in Ar found that these ferrites show strong absorption of -53.9 dB along with the broad bandwidth of 6.9 GHz within 2 to 18 GHz.

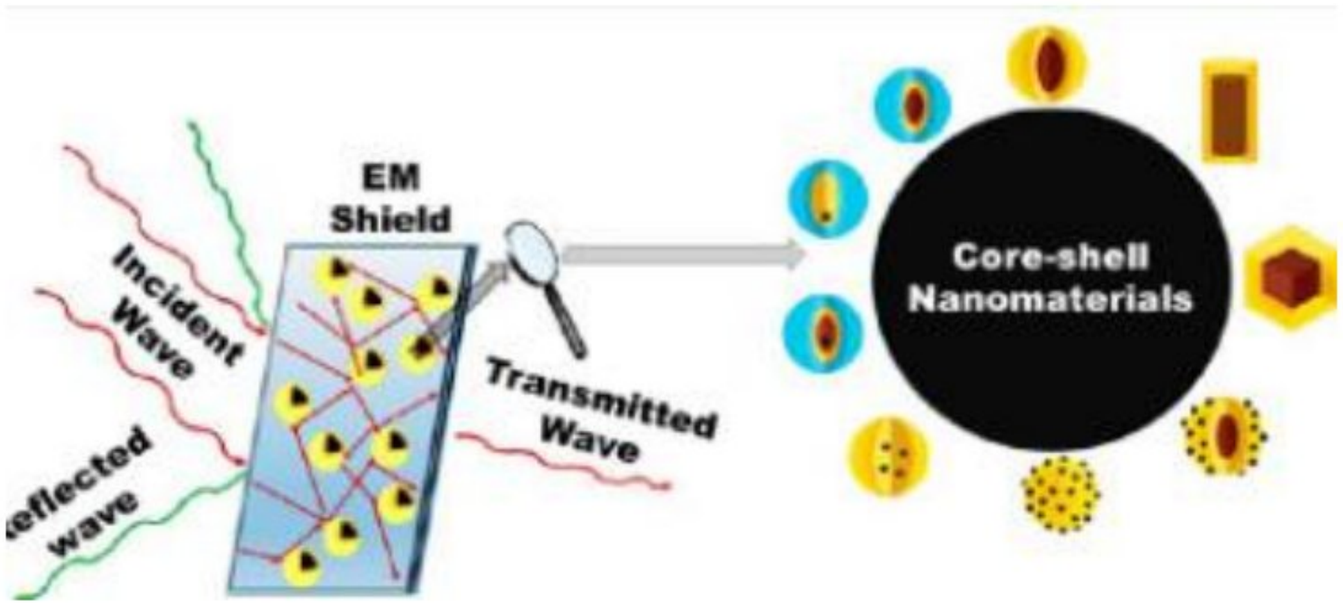

Figure 7. EMI Shielding adopted from [58].

X-band microwave absorption study was performed by K. Praveena et al. on Cr^{3+} doped Sr hexaferrite in the M-type. The reflection coefficient increased from -16 to -33 dB as the amount of Cr3 increased. Due to doping, the material showed a reflection coefficient of more than -20 dB in frequency range 9.7 and 11 GHz, while the linear increase in absorption was also visible as doping increase from x = 0.0 to 0.9. [59].

2. Biomedical Application (Magnetic Hyperthermia)

Cancer emerges as a major public health issue all over the world and it is the world's second biggest cause of death, with rising mortality rates (an expected 9.6 million deaths in 2018)[60]. Cancer is a stage of an internal disorder when some of the body cells grow uncontrollably to create complex tissue structures known as tumours. With the remarkable development in the area of oncology have been made possible by a variety of therapeutic

techniques, including surgery, radiation, chemotherapy, immunotherapy, and gene therapy. The majority of these techniques are linked to a number of serious problems that may have negative clinical consequences on healthy normal cells close to the target area [61]. Besides these, nano-carriers based drugs delivery have become increasingly popular because of their size and location specificity [62].

Hyperthermia (HPT) therapy, is very good alternative method for cancer treatment in which heat produced from magnetic nanoparticles (MNPs) are used to kill damaged cells. As a result of their small size and shape, and their surface properties, these MNPs are able to overcome biological barriers and will target tumor locations in particular; this can enhance their therapeutic efficacy by adjusting their size, shape, and surface properties.

Materials having highly saturated magnetization, like nickel, cobalt , iron, manganese, zinc, magnesium, and others oxides such as ($CoFe_2O_4$, $ZnFe_2O_4$, $NiFe_2O_4$, $MnFe_2O_4$, $CuFe_2O_4$) or iron oxides (such as magnetite and maghemite) are some of the best known MNPs for Hyperthermia (HPT) because of their effective magnetic properties [63,64].

Despite the fact that pure metals have the greatest saturation magnetization, they are highly toxic and extremely vulnerable to oxidation. Thus, such pure metal nanoparticles cannot be used in biomedical applications without appropriate surface treatment.A number of important studies have established that single domain iron oxide NPs within diameters range of 5-20 nm are interesting prospects for biomedical applications due to their biocompatibility .One of their main disadvantages is the difficulty in controlling their magnetic properties and, consequently, their heating behaviours. It has been shown, however, that particle size can have an impact on the heating behavior [66]. Specific absorption rate (SAR) measures how much heat is dissipated per unit mass of magnetic material during heating of magnetic nanoparticles in RF magnetic fields. In order to calculate this, multiply the hysteresis loop area of the material by the frequency of the applied ac magnetic field.

The loop area for magnetic nanoparticles is given by $A = \pi\mu_o^2 H^2_{max} M^2_S V.\ \omega\tau/\ 3\kappa_B T.\ (1+\omega^2\tau^2)$, In this equation, M_S is the magnetization saturation constant, μ_o is the vacuum permeability coefficient of the nanoparticles, V is the volume of the nanoparticles, and kB is the Boltzmann constant. T is for temperature, and τ is the Néel Brown relaxation expressed as $\tau = \tau_o exp(K_{eff} V)/k_B T$, Since the area of the hysteresis loop depends on magnetic parameters such as effective anisotropy, saturation magnetization and particle volume and also depends on frequency,

temperature, field and amplitude, make it very complicated to see the response of the specific absorption rate..In order to alter intrinsic magnetic properties like Ms and and effective anisotropy doping with appropriate elements (such as Cobalt ,Nickle, , Manganese in $ZnFe_2O_4$ and Strontium, Barrium in $LaMnO_3$) and creating composites out of magnetically hard and soft materials are used[66].

Strontium hexaferrite, $SrFe_{12}O_{19}$, is suitable for HPT because it has a very significant uniaxial anisotropy = 3.8 10^5 J/m^3 [68].

Hoopes et al. created ferromagnetic, dextran-coated NPs of size 100 nm and found that they supplied heat to tumour cells while having no negative effects on other cells in vitro and in vivo. The findings revealed that magnetic hyperthermic therapy considerably slowed tumor re-growth and that co-treatment with radiotherapy or chemotherapy had further effects[68,69].

Majeed et al. synthesis tunable-shell-thickness iron oxide nanospheres (15–35 nm) and treated them with silica. MNPs showed a higher specific absorption rate and more successfully eliminated cancer cells in vitro as compared to bare nanoparticles [70].

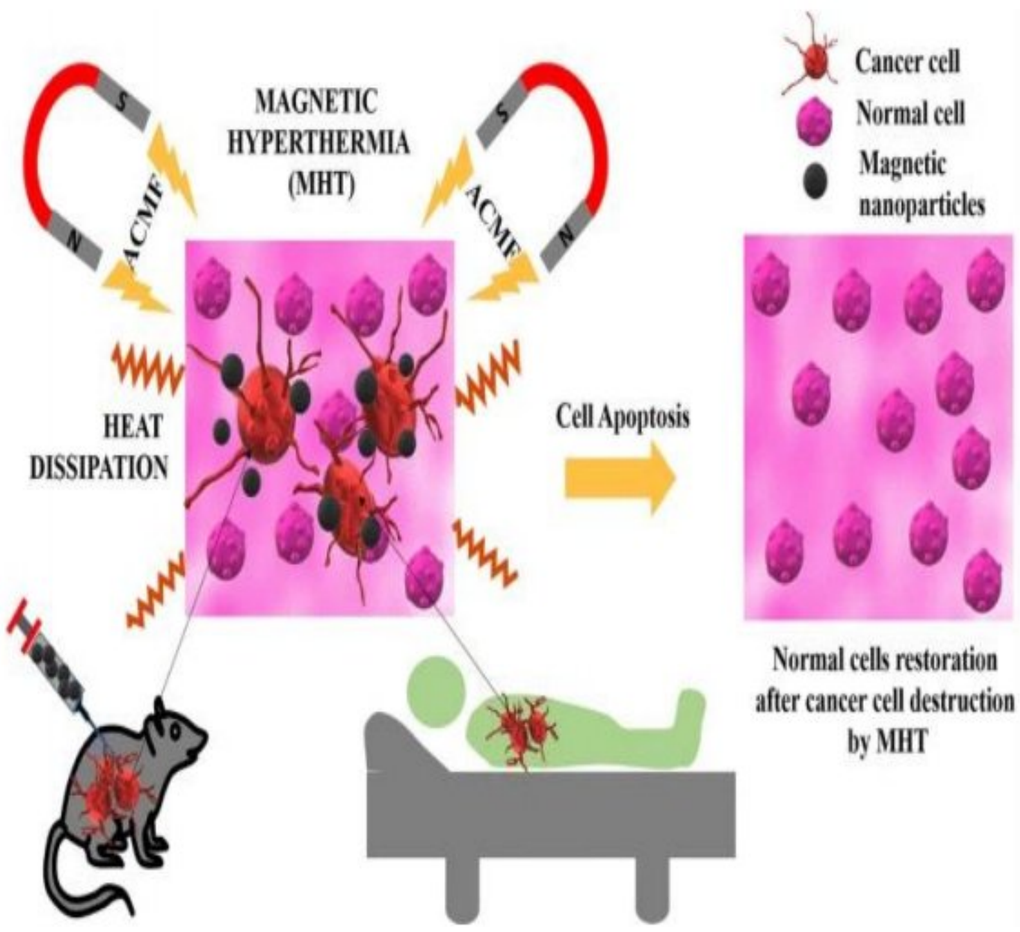

Figure 8 : Pictorial representation of magnetic nanoparticles and cancer cell destruction by MHT adoped from [71].

Liu et al. synthesised nanoflowers, a novel type of $Fe_{0.6}Mn_{0.4}O$ nanoparticles to cure cancer cells in vitro. At a modest dose of 50 g mL1, the synthesised nanoparticles efficiently heated and prevented tumour growth in vivo without damaging adjacent healthy cells [72].

Gaweda et.al uses barium ferrite ($BaFe_{12}O_{19}$) NPs for magnetic hyperthermia. [73].

3.Magnetic Recording

In the era of information, science and internet, high-density memory devices are necessary in many technological disciplines [74]. There are many different types of memories for futuristic memory devices which include RAM (resistive random-access memory) Magnetic random-access memory [75,76], phase-change memory[77] and ferroelectric memory [78]. Multiferrites are the most relevant magnetic materials and have applications in the disciplines of magnetic recording media. A study in the scientific literature shows that altering the stacking sequence of metal rich ferrites can significantly improve the intrinsic properties, especially magnetic and electrical properties. When compared with other types of ferrites, hexaferrites of the M-type (Sr, Ba, Ca, Pb) possess a very high saturation magnetization, are resistant to corrosion, have a high electrical resistivity, and possess very low dielectric losses, when compared with other types. Hexaferrites have been found to exhibit intrinsic properties that are determined by the synthesis process and by the amount of doping used in their manufacture

. In these ferroics, there are four Fe^{3+} ions with spin aligned in upward direction, give rise the total magnetic moment of 20 mB. At lower substitution levels, Ni^{2+} replaces Fe^{3+} ions from the 4f2 site while at higher substitution levels, Ni^{2+} replaces Fe^{3+} from the 12k site (upward spin). Due to the presence of Ni^{2+}, saturation magnetization and remnant values increase because the unpaired electrons have upward spin instead of the downward spin site (4f2). As the result of this the value for both the magnetization "M_S" and "M_R" will rise. Increase in net magnetization also arises on replacing the Dy^{3+} with Sr^{2+}. Ashiq et.al report the increase in coercivity (Hc) to 177 kA /m due to increase in Dy-Ni proportionin materal and rise the production of ferrous ions at the 2a lattice site , it will boosts the hyperfine interactions at the 2b & 12k sites. Increased hyperfine interactions will rise magne- tocrystalline anisotropy, resulting in increased coercivity.

The increased M_R, M_S, and coerciveness of the produced materials indicate that they can be used for magnetic recording [79].

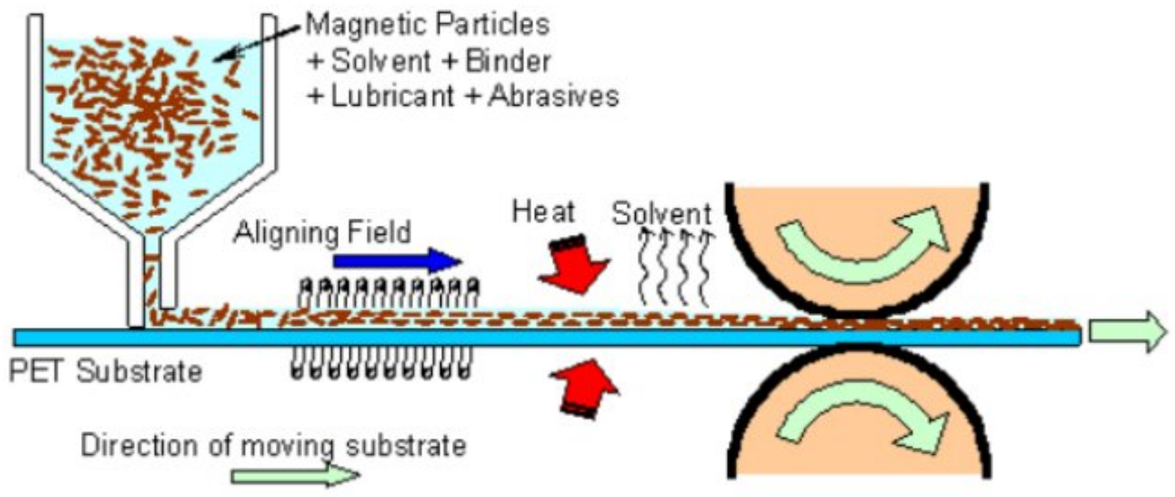

Figure 9: The processing route for particulate magnetic tape adopted from [82]

4.High Frequency Electronic Devices

Worldwide, the use of communication technology plays a vital role in the development of society. Electronic components working at high frequency have a wide range of applications Recently, Low Temperature Cofired Ceramics (LTCC) have been becoming increasingly popular for electronic components substrates because of their compactness, lightness, and high performing speed These products have become the standard for electronic components and substrates that are used on mobile devices and other personal computers. In the rapidly expanding mobile network system, cellular phones, personal digital assistants (PDAs), and personal computers are being used to transmit voice and data wirelessly. Due to their increased multifunctionality, sub-miniaturization, higher performances, frequency and excellent reliability, It was required to have a components, such as chip inductors, design to work in HF region with very large inductance.[80,81].

For fabrication of chip inductors with LTCC technology, Li et.al used (BaFe12O19) hexaferrite substituted by the Zn Ti. According to the spectrum, it can be seen that the permeability (u) of the conductive material remains relatively stable when the frequency is increased, but varies dramatically when the frequency reaches 500MHz. Due to the fact that the cut-off frequencies of ferrite exceed 500MHz, this shows that ferrites can be applied to high frequencies and that they are suitable for such applications[80].

figure below shows the internal multilayer structure the inductors. The permeability of the materials was calculated to be 13.5 at 800MHz [82].

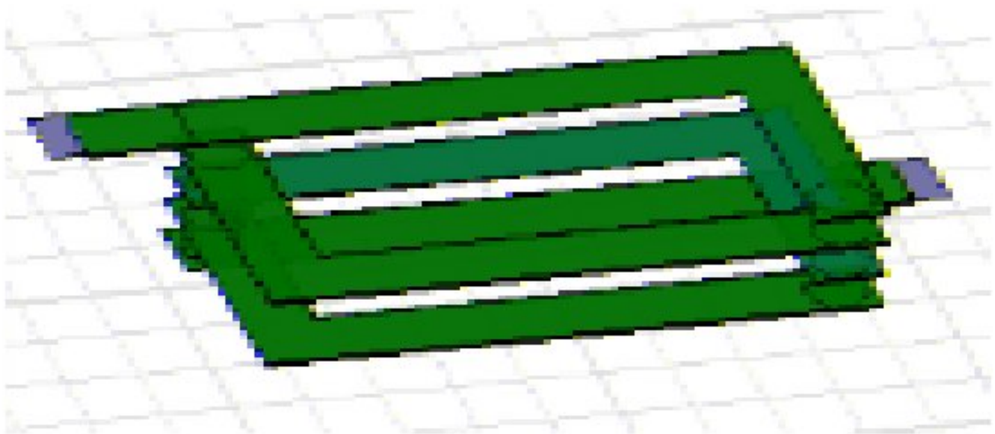

Figure 10: Multilayer structure of inductor adoped from []

Tsutaoka et.al. study the permeability and permittivity spectrum of sintered polycrystalline Barium ferrites, given by $BaFe_{12-x}(Ti\ Co)_x O_{19}$ with (x changes from 0 to 5) from RF to microwave band up to 10 GHz. The complex permeability spectra of $BaFe_{12-x}(Ti\ Co)_x O_{19}$ at (x=3) shows higher permeability about 16. According to a recent report, it has been found that composites with high magnetic permeability can be used to construct multilayer inductors at high frequencies [83].

■ REFERENCES

[1] Jeevanandam, J.; Barhoum, A.; Chan, Y. S.; Dufresne, A.;Danquah, M. K. Review on nanoparticles and nanostructured materials: history, sources, toxicity and regulations. Beilstein J. Nanotechnol. 2018, 9 (1), 1050−1074

[2] R. Valenzuela, Novel applications of ferrites, Physiother. Res. Int. 2012 (2012)

[3]V. Tsakaloudi, V.T. Zaspalis, A new Mn-Zn ferrite for high-speed data transmission applications in telecommunication networks, J. Magn. Magn Mater. 310 (2007) 2540–2542, https://doi.org/10.1016/j.jmmm.2006.11.143.

[4] T. Fujiwara, Magnetic properties and recording CHARACTERRISTICS OF barium ferrite media, IEEE Trans. Magn. 23 (1987) 3125–3130.

[5] M.P. Sharrock, L.W. Carlson, The application of barium ferrite particles in advanced recording media, IEEE Trans. Magn. 31 (1995) 2871–2876, https://doi.org/10.1109/20.490177

[8] H.N. Abdelhamid, H.F. Wu, Facile synthesis of nano silver ferrite (AgFeO2) modified with chitosan applied for biothiol separation, Mater. Sci. Eng. C 45 (2014) 438–445, https://doi.org/10.1016/j.msec.2014.08.071.

[9] Z. Karimi, L. Karimi, H. Shokrollahi, Nano-magnetic particles used in biomedicine: core and coating materials, Mater. Sci. Eng. C 33 (2013) 2465–2475, https://doi.org/10.1016/j.msec.2013.01.045.

[11] J.J. Went, G.W. Rathenau, E.W. Gorter, G.W. van Oosterhout, Hexagonal iron-oxide compounds as permanent-magnet materials, Phys. Rev. 86 (1952) 424–425.

[12] R.C . Pullar, A.K. Bhattacharya, jmmm 300: 490-499(2006).

[13] X. Sui, M.h. Kryder, B.Y . Wong, D.E. Laughlin, IEEE trans. 29: 3751(1993)

[14] J. F. Nye, Physical Properties of Crystals: Their Representation by Tensors and Matrices , Clarendon Press , Oxford, 1985 .

[15] N. A. Spaldin, M. Fiebig, Science 2005 , 309 , 391 .

[16] Kossar, Shahnaz, et al. "Ferroelectric polarization induced memristive behavior in bismuth ferrite (BiFeO3) based memory devices." Superlattices and Microstructures 148 (2020): 106726.

[17] H. Schmid, Int. J. Magn. 1973 , 4 , 337

[18] L. D. Landau and E. M. Lifshitz, Electrodynamics of continuous media (Fizmatgiz, Moscow, (1959).

[19] I. E. Dzyaloshinskii, Sov. Phys. JETP 10, 628 (1959).

[20] D. N. Astrov, Sov. Phys. JETP 11, 708 (1609).

[21] Dennis CL, Borges RP, Buda LD, Ebels U, Gregg JF, Hehn M, Jouguelet E, Ounadjela K, Petej I, Prejbeanu IL, Thornton MJ (2002) The defining lengthscales of mesomagnetism: a review. J Phys 14:11

[22] Lone et al. Nanoscale Research Letters (2019) 14:142.

[23] M.A. Almessiere, Y. Slimani, H. Güngünes¸, V.G. Kostishyn, S.V. Trukhanov, A. V. Trukhanov, A. Baykal, Impact of Eu3+ ion substitution on structural, magnetic and microwave traits of Ni–Cu–Zn spinel ferrites, Ceram. Int. 46 (2020)

[24] Aminoff G. Geol Foren Stockh Forh 1925;47:283.

[25] Adelskold V. Arkiv Kemi Min Geol 1938;12a:1.

[26] Wijn HPJ. Nature 1952;170:707.

[27] Braun PB. Nature 1952;170:708

[28]Monika Chandel, Virender Pratap Singh, Rohit Jasrotia, Kirti Singha, Rajesh Kumar. A review on structural, electrical and magnetic properties of Y-type hexaferrites synthesized by different techniques for antenna applications and microwave absorbing characteristic materials[J]. AIMS Materials Science, 2020, 7(3): 244-268.

[29] Pullar, R. C. (2012). Hexagonal Ferrites: A Review of the Synthesis, Properties and

Applications of Hexaferrite Ceramics. Prog. Mater. Sci. 57 (7), 1191–1334. Sep.2012. doi:10.1016/J.PMATSCI.2012.04.001

[30] Van Arkel AE, Verwey EJW, Van Bruggen MG. Rev Trv Chim 1936;55:331.

[31] International Centre for Diffraction Data, Newton Square, PA, USA PDF No. 84-1531 (SrFe 12O 19), 84-757 (BaFe 12O 19), 84-2046 (PbFe 12O 19).

[32] Li Z, Gao F. Can J Chem 2011;89:573.

[33] H. Kojima, in Ferromagnetic Materials, edited by E. P. Wohlfarth (North-Holland, Amsterdam,1982), p. 305.

[34] E. W. Gorter, Proc. IEEE B 104, 255 (1957).

[35] A. Moitra, S. Kim, S.-G. Kim, S.C. Erwin, Y.-K. Hong, J. Park, Defect formation energy and magnetic properties of aluminum-substituted M-type barium hexaferrite, Computational Condensed Matter (2014)

[36] A Cocherdt: J. Appl .Phys.,34,1273(1963)

[37] M.M. Hessien, M.M. Rashad, M.S. Hassan, K. El-Barawy, Synthesis and magnetic properties of strontium hexaferrite from celestite ore, J. Alloys Compd. 476 (2009) 373–378.

[38] A.M. Bolarín-Miró, F. Sánchez-De Jesús, C.A. Cortés-Escobedo, S. Díaz-De la Torre, R. Valenzuela, Synthesis of M-type SrFe12O19 by mechanosynthesis assisted by spark plasma sintering, J. Alloys Compd. 643 (2015) S226–S230.

[39] I. Novrita, Dedi, M. Azwar, Investigation of Grain exchange interaction effects on the magnetic properties of strontium hexaferrite magnets, KnE Eng. 4 (2019).

[40] T. Schmidt, D. Seifert, J. Töpfer, Phase formation and saturation magnetization of La-Zn-substituted M-type strontium ferrites, J. Magn. Magn. Mater. 508 (2020) 166887.

[41]Chen, D.-M., Li, Y.-X., Han, L.-K., Long, C., and Zhang, H.-W. (2016). Perpendicularly Oriented Barium Ferrite Thin Films with Low Microwave Loss, Prepared by Pulsed Laser Deposition. Chin. Phys. B 25, 068403–068406

[42] Kimura, T. (2012). Magnetoelectric Hexaferrites. Annu. Rev. Condens. Matter Phys. 3 (1), 93–110. doi:10.1146/annurev-conmatphys-020911-125101

[43] Khojaste khoo M., Kameli P.Structure and Magnetization of Strontium Hexaferrite (SrFe12O19) Films Prepared by Pulsed Laser Deposition ;Frontiers in Materials 8 (2021).

[44] M. Effendi, E. Nugraha, W. Tri Cahyanto, W. Widanarto, The effects of milling time on structure, magnetic properties and microwave absorption capability of strontium lanthanum ferrite compounds, J. Phys. Conf. Ser. 1494 (2020) 012042.

[45] J. Mohammed, T.T.C. Trudel, H.Y. Hafeez, D. Basandrai, G.R. Bhadu, S.K. Godara,

S.B. Narang, A.K. Srivastava, Design of nano-sized Pr3+–Co2+-substituted M-type strontium hexaferrites for optical sensing and electromagnetic interference (EMI) shielding in Ku band, Appl. Phys. A 125 (2019) 251.

[46] Z. Saeed, B. Azhdar, A novel method for synthesizing narrow particle size distribution of holmium–doped strontium hexaferrite by sol-gel auto-combustion, Mater. Res Express 7 (2020) 045006.

[47] T. Jayakumar, C.R. Raja, S. Arumugam, Structural, magnetic and optical analysis of Pb2+- and Ce3+-doped strontium hexaferrite, J. Supercond. Nov. Magn. 33 (2020) 2451–2458.

[48] M. Hassan, G.A. Ashraf, B. Zhang, Y. He, G. Shen, S. Hu, Energy-efficient de-

gradation of antibiotics in microbial electro-Fenton system catalysed by M-type

strontium hexaferrite nanoparticles, Chem. Eng. J. 380 (2020) 122483.

[49] International Centre for Diffraction Data, Newton Square, PA, USA PDF No. 84-1531 (SrFe12O19), 84-757 (BaFe 12O 19), 84-2046 (PbFe12O19).

[50] Lisnevskaya IV, Aleksandrova IA. Gel Synthesis of Hexaferrites $Pb_{1-x}La_xFe_{12-x}Zn_xO_{19}$ and Properties of Multiferroic Composite Ceramics PZT–$Pb_{1-x}La_xFe_{12-x}Zn_xO_{19}$. Nanomaterials. 2020; 10(9):1630. https://doi.org/10.3390/nano10091630

[51] P. Saini, V. Choudhary, B.P. Singh, R.B. Mathur, S.K. Dhawan, Polyaniline – MWCNT nanocomposites for microwave absorption and EMI shielding, Mater. Chem. Phys. 113 (2009) 919–926, https://doi.org/10.1016/j.matchemphys.2008.08.065.

[52] J.Z. He, X.X. Wang, Y.L. Zhang, M.S. Cao, Small magnetic nanoparticles decorating reduced graphene oxides to tune the electromagnetic attenuation capacity, J. Mater. Chem. C. 4 (2016) 7130–7140, https://doi.org/10.1039/c6tc02020h.

[53] X.F. Zhang, X.L. Dong, H. Huang, Y.Y. Liu, W.N. Wang, Microwave absorption properties of the carbon-coated nickel nanocapsules, Appl. Phys. Lett. (2006), 053115, https://doi.org/10.1063/1.2236965, 1–4.

[54] Shalom Ann Mathews, D. Rajan Babu, Analysis of the role of M-type hexaferrite-based materials in electromagnetic interference shielding, Current Applied Physics 29 (2021) 39–53.

[55] C.Y. Liu, Y.J. Zhang, Y. Tang, Z.R. Wang, H.C. Tang, Y. Ou, L. Yu, N. Ma, P.Y. Du,

Excellent absorption properties of BaFe12-x Nb x O19 controlled by multi-resonance permeability, enhanced permittivity, and the order of matching thickness, Phys.Chem. Chem. Phys. 19 (2017) 21893–21903.

[56] A.V. Trukhanov, S.V. Trukhanov, L.V. Panina, V.G. Kostishyn, D.N. Chitanov, I.S. Kazakevich, A.V. Trukhanov, V.A. Turchenko, Strong corelation between magnetic and electrical subsystems in diamagnetically substituted hexaferrites ceramics, Ceram. Int. 43 (2017) 5635–5641.

[57] Y. Zhang, et al. Journal of Magnetism and Magnetic Materials 494 (2020) 165828

[58] Yudhajit Bhattacharjee and Suryasarathi Bose Core−Shell Nanomaterials for Microwave Absorption and Electromagnetic Interference Shielding: A Review ACS Appl. Nano Mater. 2021, 4, 2, 949–972Publication Date:February 11, 2021https://doi.org/10.1021/acsanm.1c00278

[59] K. Praveena, K. Sadhana, H.L. Liu, M. Bououdina, Microwave absorption studies of magnetic sublattices in microwave sintered Cr3þ doped SrFe12O19, J. Magn. Magn Mater. 426 (2017) 604e614.

[60]Gonzales-Weimuller M, Zeisberger M, Krishnan KM (2009) Size dependant heating rates of iron oxide nanoparticles for magnetic fluid hyperthermia. J Magn Magn Mater 321:1947–1950

[61] Liauw SL, Connell PP, Weichselbaum RR (2013) New paradigms and future challenges in radiation oncology: an update of biological targets and technology. Sci Transl Med 5:173sr2

[62] Kauffman KJ, Dorkin JR, Yang JH, Heartlein MW, Derosa F, Mir FF, Fenton OS, Anderson DG (2015) Optimization of lipid nanoparticle formulations for mRNA delivery in vivo with fractional factorial and definitive screening designs. Nano Lett 15:7300–7306

[63] Sharifi I, Shokrollahi H, Amiri S (2012) Ferrite-based magnetic nanofluids used in hyperthermia applications. J Magn Magn Mater 324:903–915

[64] Abenojar EC, Wickramasinghe S, Bas-Concepcion J, Samia ACS (2016) Structural effects on the magnetic hyperthermia properties of iron oxide nanoparticles. Prog Nat Sci Mater Int 26:440–448

[65] L. A. Harris, Ph.D. Thesis, Virginia Polytechnic Institute and State University (2002).

[66] Amin Ur Rashid, Paul Southern, Jawwad A. Darr, Saifullah Awan, Sadia Manzoor, Strontium Hexaferrite (SrFe 12 O19) Based Composites for Hyperthermia Applications, Journal of Magnetism and Magnetic Materials, http://dx.

doi.org/10.1016/j.jmmm.2013.05.048 [67] Amin Ur Rashid, Paul Southern, Jawwad A. Darr, Saifullah Awan, Sadia Manzoor, Strontium Hexaferrite (SrFe 12 O19) Based Composites for Hyperthermia Applications, Journal of Magnetism and Magnetic Materials, http://dx.doi.org/10.1016/j.jmmm.2013.05.048

[68] Hoopes PJ, Tate JA, Ogden JA, Strawbridge RR, Fiering SN, Petryk AA, Barry S, Chinn P, Foreman A (2009) Assessment of intratumor non antibody directed iron oxide nanoparticle hyperthermia cancer therapy and antibody directed IONP uptake in murine and human cells. Proc SPIE Int Soc Opt Eng 23:7181:71810P. https://doi.org/10.1117/12.812056

[69] Jose et.al; Magnetic nanoparticles for hyperthermia in cancer treatment: Environmental Science and Pollution Research (2019). https://doi.org/10.1007/s11356-019-07231-2

[70] Majeed J, Pradhan L, Ningthoujam RS, Vatsa RK, Bahadur D, Tyagi AK (2014) Enhanced specific absorption rate in silanol functionalized Fe3O4 core–shell nanoparticles: study of Fe leaching in Fe3O4 and hyperthermia in L929 and HeLa cells. Colloids Surfaces B Biointerfaces 122:396–403. https://doi.org/10.1016/j.colsurfb.2014.07.019

[71] Rajan, A., Sahu, N.K. Review on magnetic nanoparticle-mediated hyperthermia for cancer therapy. J Nanopart Res 22, 319 (2020). https://doi.org/10.1007/s11051-020-05045-9

[72] Liu XL, Ng CT, Chandrasekharan P, Yang HT, Zhao LY, Peng E, Zhang H (2016) Synthesis of ferromagnetic Fe0. 6Mn0. 4O nanoflowers as anew class of magnetic theranostic

platform for in vivo T1-T2 dual mode magnetic resonance imaging and magnetic hyperthermia therapy. Adv Healthc Mater 5:2092–2104. https://doi.org/10.1002/adhm.201600357

[73] Gawęda, W. (2019). Barium Ferrite Magnetic Nanoparticles Labeled with 223Ra: A New Potential Radiobioconjugate for Targeted Alpha Therapy and Magnetic Hyperthermia. Journal of Medical Imaging and Radiation Sciences, 50(1), S3. doi:10.1016/j.jmir.2019.03.011

[74] R. Waser, M. Aono, Nonoionics-based resistive switching memories, Nat.

Mater. 6 (2007) 833e840.

[75] J. Åkerman, Toward a universal memory, Science 308 (2005) 508e510.

[76] M. Wuttig, N. Yamada, Phase-change materials for rewriteable data storage, Nat. Mater. 6 (2007) 824e832.

[77] V. Garcia, S. Fusil, K. Bouzehouane, S. Enouz-Vedrenne, N.D. Mathur, A. Barthelemy, M. Bibes, Giant tunnel electroresistance for non-destructive

readout of ferroelectric states, Nature 460 (2009) 81e84.

[78] Wu, C., Liu, Q., Wang, Y., Chen, J., Qi, B., Zhang, H., & Liu, Y. (2019). *Room-temperature nonvolatile four-state memory based on multiferroic Sr3Co2Fe21.6O37.4. Journal of Alloys and Compounds, 779, 115–120.* doi:10.1016/j.jallcom.2018.11.256

10.1016/j.jallcom.2018.11.256

[79] Muhammad Naeem Ashiq, Muhammad Javed Iqbal, Muhammad Najam-ul-Haq, Pablo Hernandez Gomez, Ashfaq Mahmood Qureshi,Synthesis, magnetic and dielectric properties of Er–Ni doped Sr-hexaferrite nanomaterials for applications in High density recording media and microwave devices,Journal of Magnetism and Magnetic Materials,Volume 324, Issue 1,2012,Pages 15-19, ISSN 0304-8853, https://doi.org/10.1016/j.jmmm.2011.07.016.

[80] Yuanxun Li, Yingli Liu, Shengjun Yuan, Huaiwu Zhang, Hai Nie, & Jianhong Kang. (2010). The design and fabrication of LTCC chip inductors for high frequency applications based on barium ferrites. 2010 11th International Conference on Electronic Packaging Technology & High Density Packaging. doi:10.1109/icept.2010.5582663

[81] Heo, Keun; Lim, JuHwan; Mun, JeDo; Hwang, SungWoo.“Characterization and wideband modeling of miniaturized LTCC helical inductors,” IEEE Microwave and Wireless Components Letters, Vol. 17, No 3(2007), pp .160-162.

[82] Yuanxun Li, Yingli Liu, Shengjun Yuan, Huaiwu Zhang, Hai Nie and Jianhong Kang, "The design and fabrication of LTCC chip inductors for high frequency applications based on barium ferrites," 2010 11th International Conference on Electronic Packaging Technology & High Density Packaging, Xi'an, 2010, pp. 906-908, doi: 10.1109/ICEPT.2010.5582663.

[83] Takanori Tsutaoka, Aiko Tsurunaga, Nobuyoshi Koga, Permeability and permittivity spectra of substituted barium Ferrites BaFe12−x(Ti0.5Co0.5)xO19(x=0 to 5),Journal of Magnetism and Magnetic Materials,Volume 399,2016,Pages 64-71,ISSN 0304-8853,https://doi.org/10.1016/j.jmmm.2015.09.032.